

# Preparation and Property of Raspberry-Like AS/SiO<sub>2</sub> Nanocomposite Particles

Hong Zhang, Zhixing Su, Peng Liu, Fangzhi Zhang

*Institute of Polymer Science and Engineering, College of Chemistry and Chemical Engineering, Lanzhou University, Lanzhou 730000, People's Republic of China*

Received 24 February 2006; accepted 27 April 2006

DOI 10.1002/app.25172

Published online in Wiley InterScience (www.interscience.wiley.com).

**ABSTRACT:** Surfactant-free poly(acrylonitrile-co-styrene)/silica (AS/SiO<sub>2</sub>) nanocomposite particles was synthesized in the presence of cheap, commercially amorphous aqueous silica sol at ambient temperature. Thermogravimetric analysis (TGA) indicated silica contents ranging from 5 wt % to 29 wt %, depending on reaction conditions. Particle size distributions and morphologies were studied using dynamic light scattering (DLS) and transmission electron microscopy (TEM), which clearly showed that most of the colloidal nanocomposites comprised approximately spherical particle with raspberry-like morphology and relatively narrow size distributions. The optical clarity of solution-cast nanocompo-

site films was assessed using UV-vis spectrometer, with high transmission being obtained over the whole visible spectrum. Differential scanning calorimetry (DSC) studies showed that the glass transition temperature of AS/SiO<sub>2</sub> nanocomposites can be higher than the corresponding pure AS, resulting from the hydrophilicity of the nanometer silica. The robustness and simplicity of this method may make large-scale manufacture of this nanocomposite possible. © 2007 Wiley Periodicals, Inc. *J Appl Polym Sci* 104: 415–421, 2007

**Key words:** raspberry-like structure; silica; nanocomposite spheres; poly(acrylonitrile-co-styrene)

## INTRODUCTION

In recent years, polymer-inorganic nanocomposites have become the subject of rapidly growing interest. Intimate mixing of polymer with inorganic particles on a nanoscale can lead to unusual properties,<sup>1–4</sup> obviously, which cannot be obtained simply by combining the polymeric component with the inorganic phase at the macroscopic level. Among the inorganic particle materials, silica is one of the most popular candidate, since it has great potential application in many industrial areas such as paints, catalysis, drug delivery, composite materials and so on.<sup>5–8</sup> In the literature, polymer nanocomposites were prepared by creating or modifying the inorganic phase in the presence of surfactant,<sup>9</sup> stabilizer,<sup>10,11</sup> reactive coupling agent,<sup>5,12</sup> or preformed polymer chains.<sup>13,14</sup>

*In situ* polymerization in the presence of existing porous or colloid silica is becoming increasingly common.<sup>15–17</sup> In the past few years, there has been increasing interest in the synthesis of particulate or colloidal organic/inorganic hybrids, and a comprehensive review of colloidal nanocomposites has been published.<sup>18</sup> For example, Bourgeat-Lami and Lang<sup>10</sup> have synthesized the polystyrene/silica composite

particles by nonaqueous dispersion polymerization of styrene in alcoholic media in the presence of surface-functionalized silica particles, using polymeric stabilizers such as poly(*N*-vinylpyrrolidone), which can lead to formation of nanocomposite particles or core-shell morphologies (silica cores, polystyrene shells), depending on the diameter of the particles of silica. Tissot et al.<sup>5,12</sup> described the coating reaction of polystyrene latex with a silica layer by using a silane coupling agent to improve the compatibility of organic core and inorganic shell materials. Luna-Xavier and Bourgeat-Lami et al.<sup>11,18</sup> prepared the poly(methyl methacrylate)/silica nanocomposite particles. Pu et al.<sup>19</sup> prepared monolithic poly(methyl acrylate)/silica composites by dispersing surface-modified silica particles in methyl acrylate, followed by polymerization of the monomeric continuous phase. However, most of these works have a common peculiarity, i.e., it is necessary to pretreat the surface of silica particles in the former process and to repeat the filtration/wash/redispersion cycles in the latter process, which is very tedious and energy-consuming.

To work out these problems, Armes and co-workers<sup>20–26</sup> proposed a novel method to synthesize a series of raspberry-like vinyl polymer/SiO<sub>2</sub> organic-inorganic hybrid microspheres. In their method, 4-vinylpyridine (4-VP) was used as an auxiliary monomer. Thus, the basic property of the amino group from 4-VP could interact with the acidic property of the

Correspondence to: Z. Su (suzx@lzu.edu.cn).

hydroxyl groups from nanosilica surface to enhance the compatibility between the organic and inorganic phase. Tiarks et al.<sup>27</sup> reported in detail the preparation of lattices with silica nanoparticles as surfactants and fillers via miniemulsion polymerization. They had used nonionic surfactant, anionic surfactant, and cationic surfactant as traditional surfactant in miniemulsion polymerization or silica itself as "pickering surfactant" in soapless polymerization. Depending on the reaction conditions and the surfactants employed, different hybrid morphologies were obtained. It turned out to be a meaningful supplement to the Arme's work. Most recently, Chen et al.<sup>28</sup> used 1-vinylimidazole (1-VID) as an auxiliary monomer to successfully prepare raspberry-like PMMA/SiO<sub>2</sub> nanocomposite particles via surfactant-free method. The acid–base interaction between the silica surface and 1-VID promoted the formation of nanocomposite particles, which was similar to Arme's work. While Wu and coworkers<sup>29</sup> also reported another cationic auxiliary monomer, 2-(methacryloyl)ethyltrimethylammonium chloride (MTC), which improved the adsorption between the inorganic and organic phase via electrostatic interaction between MTC and nanosilica particles. In the opinion of Wu and coworkers, electrostatic interaction between negatively charged silica and positively charged MTC was strong enough for the formation of long-stable hybrid microspheres. This work substantially broadened and extended the scopes of such subject system. Further work and more kinds of polymer–inorganic nanocomposite particles with this morphology will be prepared and studied in this area.

Although some papers have reported on this subject, as mentioned earlier, the main objective of our present work is to try to obtain a new nanocomposite by this new method with cheap materials and to explain the formation mechanism of nanocomposite particles. We first synthesized the raspberry-like morphological poly(acrylonitrile-co-styrene)/silica (AS/SiO<sub>2</sub>) nanocomposite particles with well-defined and relatively narrow size distribution at ambient temperature. The latex was long-stable in the presence of an aqueous amorphous silica sol and required neither expensive special auxiliary comonomer nor surfactant. This convenient route was different from the traditional sol–gel process by hydrolysis tetraethoxysilane, and the average size, morphology, and silica content of the nanocomposite particles could be easily controlled. The interaction between acrylonitrile and silica was the substantial "bind" to connect the organic phase with inorganic component, which was most likely responsible for nanocomposite particle formation. We believe there has been no report on preparing AS/SiO<sub>2</sub> hybrid microspheres with raspberry-like morphology, using this method.

## EXPERIMENTAL

### Materials

Styrene (ST) and acrylonitrile (AN) were purchased from Lanzhou Chemical (China), purified by treating it with 5 wt % aqueous NaOH to remove the inhibitor, and then washed until pH = 7. It was dried over by anhydrous calcium chloride for 24 h and then stored at low temperature prior to use. Amorphous aqueous silica sol was supplied by Qingdao Ocean Chemical (China) (ca. 20 nm, pH = 10.0, 20 wt %). Ammonium persulfate (APS), *N,N,N',N'*-tetramethylethylene-diamine (TEMED), isopropyl alcohol (IPA), hydrogen fluoride (HF), *N,N*-dimethylformamide (DMF) and other reagents were analytic grade and were used as received.

### Synthesis of nanocomposite particles

Copolymer/silica nanocomposite particles were prepared by free radical copolymerization of AN with ST in the presence of amorphous aqueous silica sol and IPA mixture media. A typical synthetic process was described as follows: the amorphous aqueous silica sol (33 mL, equivalent to 7.5 g of dry weight silica), IPA (25 mL), and water (25 mL) were mixed in a 250-mL three-necked round-bottom flask equipped with mechanical stirrer. The pH of the mixture solution was adjusted to the required value using aqueous NaOH or HCl solution. This reaction mixture was stirred at room temperature for 10 h before the comonomer was added. Then an amount of AN (1.6 mL, 1.25 g) and ST (4.2 mL, 3.75 g) were mixed into the reaction system. After 30 min, APS (initiator, 50.0 mg; 0.2 mmol; 1.0 wt % based on total comonomer mass) dissolved in water and TEMED (25.0 mg; the APS/TEMED molar ratio was unity) dissolved in water were separately degassed and added to the reaction vessel. The reaction mixture was stirred at 25°C for 24 h under a slow stream of N<sub>2</sub>. The resultant milk-white colloidal dispersions were purified by several centrifugation–redispersion cycles, with each successive supernatant being carefully decanted and replaced with deionized water, until no excess silica sol was observed by transmission electron microscopy (TEM). A series of hybrid microspheres were synthesized using different reaction conditions, as summarized in Table I.

### Characterization of AS/SiO<sub>2</sub> nanocomposite materials

Particle size analysis of nanocomposite microsphere

The diameter of the latex particles was determined by dynamic light scattering (DLS) using B1-200SM. All measurements were carried out at room temperature at a fixed angle of 90° on highly diluted

**TABLE I**  
**Summary of AS/SiO<sub>2</sub> Nanocomposite Particles Obtained at Different Conditions**

Run	AN/ST (mass/mass)	SiO <sub>2</sub> /mon (mass/mass)	pH value	T (°C)	Colloid stability <sup>a</sup>	Particle size (nm)		SiO <sub>2</sub> (wt %)
						DLS	TEM	
1	ST	1.5/1	10	25	–			
2	5/95	1.5/1	10	25	+–	460	180	1.7
3	15/85	1.5/1	10	25	+	410	170	4.8
4	25/75	1.5/1	10	25	+	233	140	17.4
5	35/65	1.5/1	10	25	+	214	130	22.3
6	45/55	1.5/1	10	25	+	189	120	28.5
7	25/75	0.5/1	10	25	+–			
8	25/75	1.0/1	10	25	+	271	165	9.7
9	25/75	2.0/1	10	25	+	182	110	22.0
10	25/75	2.5/1	10	25	+	175	105	23.1
11	25/75	3.0/1	10	25	+	176	105	23.5
12	25/75	1.5/1	7	25	–			
13	25/75	1.5/1	8	25	+	342	230	10.1
14	25/75	1.5/1	9	25	+	271	175	12.3
15	25/75	1.5/1	11	25	+	225	140	19
16	25/75	1.5/1	12	25	+	212	135	21.6
17	25/75	1.5/1	10	40	+	324	125	8.9

<sup>a</sup> +, stable colloid; +–, metastable colloid; –, unstable system.

aliquots taken from the redispersed solution to obtain the intensity-average diameters of the particles. Each analysis was repeated three times to give the average particle size.

#### Chemical composition analysis of hybrid materials

Thermogravimetric analysis was performed using a WCT-2C instrument. Nanocomposite dispersions were dried to yield dried powder. These powders were heated from room temperature to 800°C at a scan rate of 20°C/min in nitrogen, and the observed mass loss was attributed to the quantitative pyrolysis of the copolymer component. Assuming that the incombustible residues were pure silica, the silica content of the hybrid materials was calculated after correcting for loss of surface moisture of the silica sol at elevated temperature.

#### Morphology of nanocomposite particles

Transmission electron microscopy (HITACHI H-600) operating at 100 kV was used to observe the morphologies of nanocomposite particles. The nanocomposite particles dispersions were diluted, ultrasonized, and then dried onto carbon-coated copper grids for examination.

#### Other characterization methods

The glass transition temperature ( $T_g$ ) of the nanocomposites was determined by differential scanning calorimetry (Perkin–Elmer Sapphire), between 40 and 170°C at a heating rate of 10°C/min. A nitrogen

purge was applied. Transparencies of solution-cast films were assessed using Perkin–Elmer Lambda 35 UV–vis spectrometer in the 250–800 nm range. The molecular weights of the selected copolymer were obtained by static light scattering (SLS) using B1-200SM.

## RESULTS AND DISCUSSION

### Effect of the acrylonitrile–styrene comonomer ratio

The effect of the AN–ST comonomer mass ratio on the hybrid microspheres was investigated, and it is summarized in Table I (Runs 2–6) and illustrated in the Figure 1 for clear comprehension. It can be seen that the stability of the colloid system varied with the ratio of AN/ST. At first, we used the pure ST monomer; there was no stable colloid system obtained which could not be redispersed by shaking and had ill-defined particle morphology (Table I, Run 1). However, when using a minor amount of AN (5 wt %) in the reaction system, metastable milk-like dispersion was obtained. In this case, very large but metastable particles were in coexistence with a majority of free silica particles. In the milk-like dispersion colloid almost bare AS particles were obtained [see Fig. 4(c)]. After the centrifugation–redispersion process, thermogravimetric analysis (TGA) confirmed that the silica content in the nanocomposite particles was only ~ 1.7 wt %. With the increasing ratio of the AN/ST, the final silica content increased and the nanocomposite particle became well-defined and the average size decreased. When the monomer became all of AN, the silica content

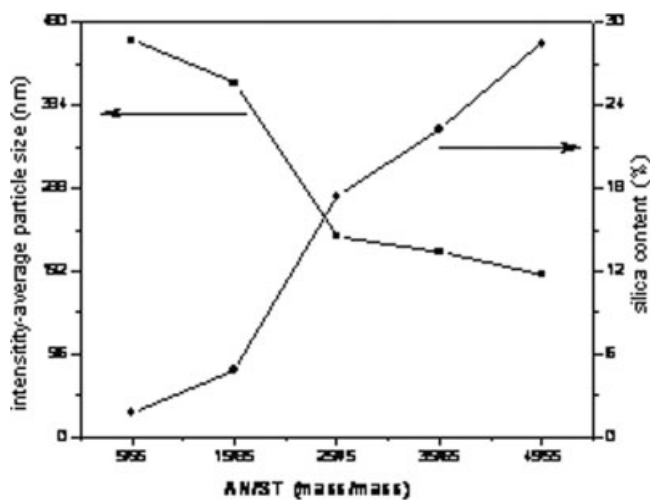


**Figure 1** Effect of AN/ST comonomer ratio on the particle size and silica content.

was over 40 wt % and the diameter of the nanocomposite particles was dramatically decreased, while its morphology was somewhat different with the AS/SiO<sub>2</sub> nanocomposite particles, which was another subject. In this present study, with the AN/ST ratio increasing from 15/85 to 45/55, the final silica content of the hybrid microspheres increased from 4.8 wt % to 28.5 wt %, and the average particle size decreased from 410 to 189 nm, respectively, (see Fig. 1, Runs 2–6 in Table I). These results were coincident with the results reported by Armes and coworkers<sup>21,22</sup> when using 4-VP as auxiliary monomer or by Wu and coworkers<sup>28,29</sup> when using 1-VID or MTC as auxiliary monomer. These results indicated there was interaction between acrylonitrile and silica, and some phenomena in the experiments discussed next two section also partly indicated the interaction (see later).

#### Effect of the initial silica and isopropyl alcohol charge

Figure 2 (Table I, Runs 8–11 and 4) illustrated the changes in the sizes of both nanocomposite particles and silica content adsorbed on nanocomposite particles as a function of the mass ratio of SiO<sub>2</sub>/monomer. It was found that the average particle size ranged from 271 to 176 nm and silica content ranged from 9.7 wt % to 23.5 wt %, respectively, with increasing initial silica charged. It suggested that silica particles acted as “pickering emulsifier”<sup>30</sup> and had the same behavior as traditional emulsifier. But when the mass ratio of SiO<sub>2</sub>/monomer was over 2.5/1, both the diameters and final silica contents of the microspheres hardly changed with the amount of initial silica charged (see Fig. 2 and Table I, Runs 10–11). This was inconsistent with the results re-

ported by Armes and coworkers.<sup>21,22</sup> Perhaps it could be explained that the interaction between AN and silica was too weak to adsorb more silica particles when the amount of AN was constant. Metastable nanocomposite particles were obtained when the mass ratio of SiO<sub>2</sub>/monomer minimized to 0.5/1 (Run 7, in Table I). A controlled experiment without silica sol was carried out. It was found that only macroscopic precipitates were obtained (not shown in Table I).

In our experiment, isopropyl alcohol (IPA) played a crucial role in the whole reaction process. It can be proved that before charging the comonomer and initiator, the reaction mixture media (IPA, silica sol, and water) should be stirred over 10 h, which was necessary for formation of well-defined nanocomposite microspheres. The media stirred for enough time perhaps subtly influenced the surface chemistry of silica sol, which destroyed the interparticle hydrogen bonding of the silica, and so destroyed the molecular network of the silica sol. Thus, this kind of media led to silica incorporation within the growing copolymer particles easily. But, surprisingly, both the silica content and average particle diameter of the nanocomposite particles proved to be insensitive to the amount of the initial IPA charged, when its content varied from 20 wt % to 40 wt % in the cosolvent of the reaction mixture media.

#### Effects of pH value and reaction temperature

Since the surface chemistry of the nanosilica particle and the zeta potential of the silica sol were strongly influenced by the pH value, the pH value of the reaction system represented another parameter that had a pronounced crucial impact on the formation of nanocomposite particles. It turned out that stable nanocomposite particles were obtained only under

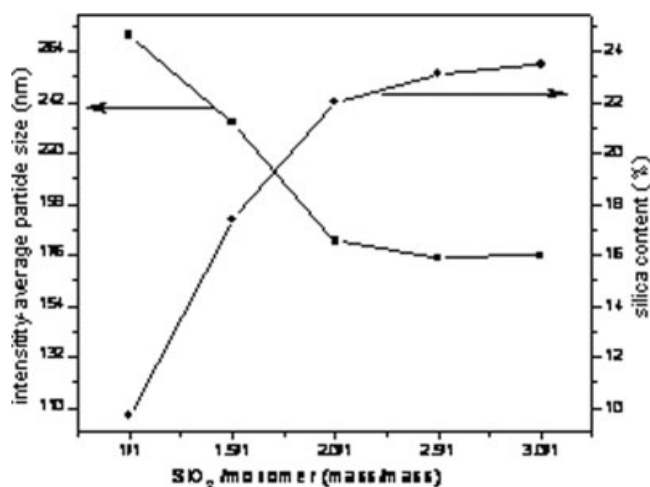


**Figure 2** Effect of initial charged-silica on the particle size and silica content.

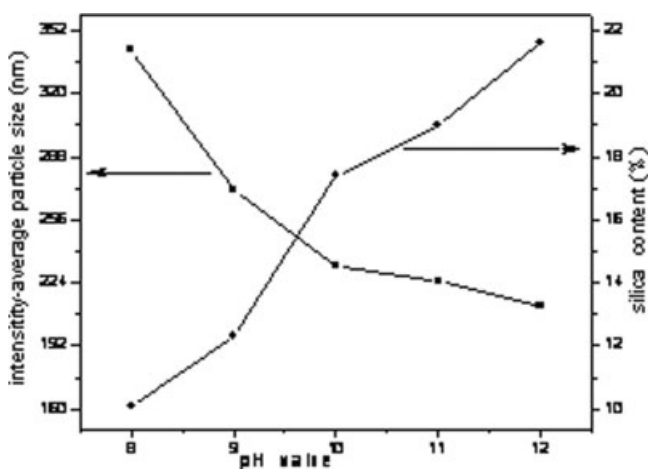


**Figure 3** Effect of pH values on the particle size and silica content.

alkaline conditions. If pH value was below 7, only large, polydisperse aggregates and large amounts of coagulum could be obtained (see Table I, Run 12). Figure 3 (Runs 13–16 and 4, in Table I) clearly demonstrated the influence of pH value of the system on the nanocomposite particles. In the basic range, the lower the pH value, the lesser the silica content in the nanocomposite particle, and the larger nanocomposite particles. This may be pertinent that at the lower pH value, the silica sol was relatively low zeta potential and was prone to decrease the reactivity of the surface chemistry of the silica particles. So, the interaction between silica and AN also decreased. As a result, the silica content on the nanocomposite particles would be decreased and the average particle size would be increased, since much fewer silica particles acted as “pickering emulsifier.”

The average particle size and final silica content were also rather sensitive to the reaction temperature: copolymerization of AS/SiO<sub>2</sub> at 40°C produced nanocomposite particles that were somewhat larger, with significantly lower silica content than that obtained for particles synthesized at 25°C (compare Runs 4 and 17 in Table I). With the increasing of reaction temperature, it was inclined to hardly obtain long-term colloid stabilities of the nanocomposite dispersions. When the copolymerization of AS/SiO<sub>2</sub> carried out over 60°C and without the TEMED in the initiator system, only macroscopic precipitates were obtained. From these phenomena, it seemed that the interaction between the silica and the AN was not sufficiently strong to promote efficient nanocomposite formation under these conditions.

### Morphology of the nanocomposite particles

Figure 4 displayed some representative transmission electron micrographs of the AS/SiO<sub>2</sub> nanocomposites. From these images, one could see a distinct raspberry-like morphology. The hybrid microspheres obtained at a mass ratio of AN/ST = 25/75 (Table I, Run 4) were approximately spherical and had a rather narrow size distribution, which could be seen from the Figure 4(a, b). The surface roughness was caused by amorphous silica particles protruding from the particle surface. But when the mass ratio of AN/ST decreased to 5/95 [see Fig. 4(c), Table I, Run 2], there was some tendency for the formation of metastable hybrid microsphere. It may be because that less AN resulted in few silica particles adsorbed onto the polymer surface, which was insufficient to stabilize the hybrid microsphere. In Figure 4(c), it was found that the silica on the copolymer micro-

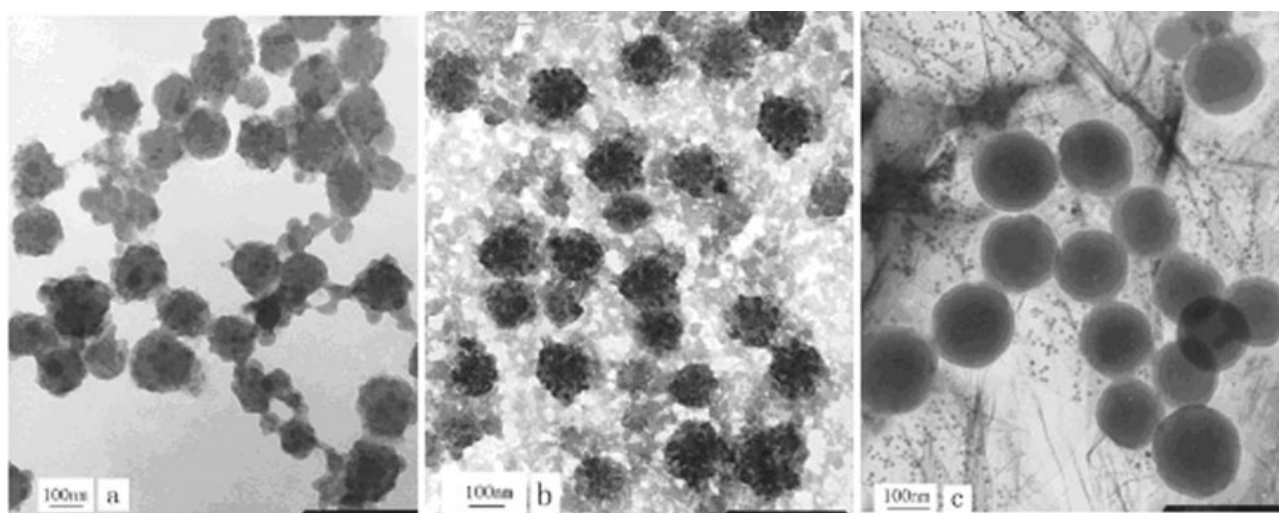


**Figure 4** Representative TEM image of obtained nanocomposite particles; (a) Run 4 with raspberry-like morphology; (b) Run 4 with raspberry-like morphology before centrifugation–redispersion cycles; (c) Run 2 shows the imperfect stabilization and very low silica content if AN/ST ratio is low.

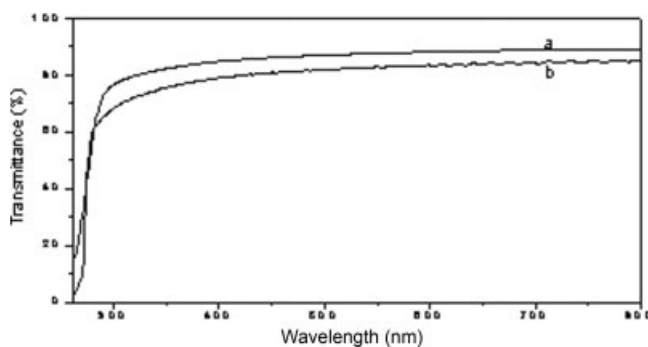


**Figure 5** Optical absorption spectra of 20- $\mu\text{m}$  films; (a) HF-etched AS-SiO<sub>2</sub> obtained the pure AS film; (b) AS-SiO<sub>2</sub> (Run 8 silica content 9.7 wt %) film.

spheres was very poor though the particle size seemed rather uniform, and the serious flocculation soon occurred.

The stability and the size distribution of this system were further confirmed by the discrepancy between the DLS and TEM studies. Generally, the diameter of nanocomposite particles from DLS was "oversize" relative to the one from TEM, since the DLS technique was much more sensitive to the presence of large particles.<sup>26</sup> In most cases, the difference in mean particle diameter obtained from DLS and TEM studies was relatively small (see Table I), but in a few cases large discrepancies were observed. It indicated that this dispersion was weakly flocculated and had a rather broad size distribution of the system (e.g., Table I, Run 2).

### Optical clarity of nanocomposite film

Film formation was not anticipated for the copoly (AN-ST)/silica nanocomposite prepared in this study. However, the properties of the nanocomposite after film formation rely on the fact that the polymer and inorganic nanoparticles are homogeneously blended on the length scales exceeding the original macroscopic hybrid structure.<sup>27</sup> In line with this idea, for the purpose of studying the dispersion of silica particles within the copolymer matrix, we prepared AS-based nanocomposite film using wet film spreader and micrometer caliper by solvent casting at ambient temperature. Two kinds of films were prepared: the first one was pure AS film by etching AS/SiO<sub>2</sub> nanocomposite (Run 8, in Table I, silica content 9.7 wt %) then dissolving it in DMF to prepare AS film, and the controlled film thickness was 20  $\mu\text{m}$ . The second one was a nanocomposite film by dissolving AS/SiO<sub>2</sub> nanocomposite (Run 8, in Table I, silica content 9.7 wt %, just mentioned above) in DMF to prepare AS/SiO<sub>2</sub> film (AS/SiO<sub>2</sub> nanocomposite can soluble in DMF), and the film thickness was also 20  $\mu\text{m}$ . These films exhibited reasonable transparency, gloss, and somewhat break-

ability as judged by the naked eye. The optical clarity of the nanocomposite film was assessed using UV-vis spectroscopy. As shown in Figure 5, the two spectra were very similar, and the degree of light adsorption was relatively low over the entire visible wavelength range (400–800 nm). The result of the spectroscopy indicated that the silica particles were well dispersed and retained small size within the nanocomposite film, because appreciable flocculation would inevitably lead to significant light scattering and hence reduced transmittance.

### Glass transition temperature of the nanocomposite material

DSC was performed on some selected nanocomposite formulations, and these results were in contrast to the copolymer without silica. As clearly shown in Figure 6, the pure AS obtained from the HF extraction of Run 8 in Table I was used as a reference material, which had a  $T_g$  of around 102°C, while in the case of AS/SiO<sub>2</sub> nanocomposite (Runs 3, 8, and 4, silica content 4.8 wt %, 9.7 wt %, and 17.4 wt %) the data was shifted to 110, 117, and 119°C, respectively. Because the glass transition temperature for the ST and AN homopolymer are both approximately 100°C, the AN/ST ratio has little effect on the  $T_g$  of the copolymer. The molecular weight of the selected copolymer/SiO<sub>2</sub> nanocomposite had no significant difference as judged by static light scattering (SLS) studies (usually about  $3.7 \times 10^4$  g/mol, samples etched by HF). So, it was clear that the shift of the  $T_g$  only resulted from the nature of the nanoscale silica. The glass transition temperature of a polymer corresponds to the onset of significant segmental chain motion; hence this property is sensitive to the local environment of the polymer chains. In our work, it was clearly observed that with the increase of silica content on the nanocomposite, the  $T_g$  of the corresponding material dramatically increased. This shift was usually interpreted in terms of reduced mobility of the polymer chain due to their interaction

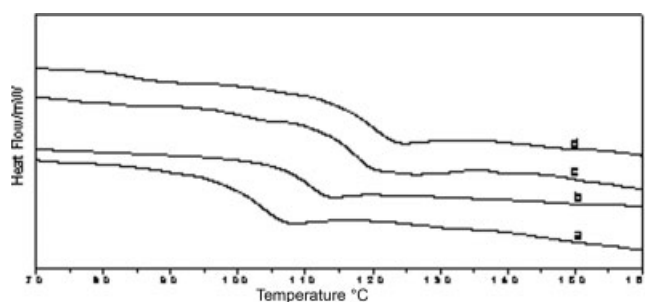


**Figure 6** DSC curves of representative nanocomposites; (a) HF-etched AS-SiO<sub>2</sub> obtained the pure AS ( $T_g = 102^\circ\text{C}$ ); (b) AS-SiO<sub>2</sub> (Runs 3, silica content 4.8 wt %,  $T_g = 110^\circ\text{C}$ ); (c) AS-SiO<sub>2</sub> (Run 8, silica content 9.7 wt %,  $T_g = 117^\circ\text{C}$ ); (d) AS-SiO<sub>2</sub> (Run 4, silica content 17.4 wt %,  $T_g = 119^\circ\text{C}$ ).

between copolymer and the inorganic phase. This could suggest that these composite materials possessed very fine grain and high degree of dispersion, interpenetrating copolymer/silica morphologies. Arrighi et al.<sup>31</sup> have reported that adding ultrafine silica nanocomposites to ST-butadiene rubber can either have little effect on the  $T_g$  or lower the  $T_g$ , depending on the properties of the silica (surface is organophilic). Thus, it was a satisfactory explanation for our results, because the used unmodified silica was of great hydrophilicity.

### Formation mechanism of the AS/SiO<sub>2</sub> nanocomposite particles

ST monomer is insoluble in water, while AN monomer is only sparingly soluble in water. Thus, the solubility of the organic phase was neglected, which was similar to the opinion of Wu and coworkers<sup>28</sup> In the present work, it was quite likely that the silica sol acted as a "picking emulsifier"<sup>30</sup> for the AN-ST droplets prior to polymerization. This emulsification was very important for the formation of colloidal stable nanocomposite particles. In the meantime, other phenomena illustrated that AN also acted as an essential role in the formation of nanocomposite particle. Therefore, on the basis of all the experimental results and discussion, it seemed that AN acted as a "binder" to connect the organic phase with inorganic silica particles. We suggested that nanocomposite particle with raspberry-like morphology was obtained by cooperation of silica with AN directly from the polymerization of silica-stabilized monomer droplets.

### CONCLUSIONS

In summary, this was the first report on preparation of raspberry-like morphological AS/SiO<sub>2</sub> nanocomposite particle by a simple protocol at around ambient temperature. What's more, it will be preferable that the whole process is economical and simple without recourse to expensive, special and auxiliary comonomer or adding any surfactant. Depending on the precise formulation, the average particles size and the final silica contents of the hybrid microspheres from 410 to 180 nm and 5 to 29 wt % respectively, can be obtained. Both the AN and the silica sol were essential for the formation of colloidal stable nanocomposite particles. The influence of other parameters such as the pH value, reaction temperature, and the reaction media of the experiment were also studied. On the basis of experimental results and discussion, we believe that the raspberry-like particles were obtained directly from the polymerization of silica-stabilized monomer droplets. The hydrophilic silica beads acted as "picking emulsifier" to stabilize the nanocomposite particles.

According to the UV-vis spectra and DSC studies, with the increasing of silica content in the AS-based hybrid materials, the optical clarity of the nanocomposite film reduced little, while their glass transition temperature increased dramatically. Since adjusting the glass transition temperature of organic phase could control many properties of nanocomposite particles and the reaction media is aqueous, these nanocomposites are of great potential interest as environmentally friendly tough, abrasion-resistant, transparent materials.

### References

1. Marinakos, S. M.; Shultz, D. A.; Feldheim, D. L. *Adv Mater* 1999, 11, 34.
2. Beecroft, L. L.; Ober, C. K. *Chem Mater* 1997, 9, 1302.
3. Chen, B. K.; Chiu, T. M.; Tsay, S. Y. *J Appl Polym Sci* 2004, 94, 382.
4. Krishnamoorti, R.; Giannelis, E. P. *Macromolecules* 1997, 30, 4097.
5. Tissot, I.; Novat, C.; Lefebvre, F.; Bourgeat-Lami, E. *Macromolecules* 2001, 34, 5737.
6. Lu, Y.; McLellan, J.; Xia, Y. *Langmuir* 2004, 20, 3464.
7. Kamata, K.; Lu, Y.; Xia, Y. *J Am Chem Soc* 2003, 125, 2384.
8. Graf, C.; Vossen, D.; Imhof, A. *Langmuir* 2003, 19, 6693.
9. Reculosa, S. Poncet-Legrand, C.; Ravaine, S.; Mingotand, C.; Duguet, E.; Bourgeat-Lami, E. *Chem Mater* 2002, 14, 2354.
10. Bourgeat-Lami, E.; Lang, J. *Colloid Interface Sci* 1998, 197, 293.
11. Luna-Xavier, J. L.; Bourgeat-Lami, E.; Guyot, A. *Colloid Polym Sci* 2001, 279, 947.
12. Tissot, I.; Reymond, J. P.; Lefebvre, F.; Bourgeat-Lami, E. *Chem Mater* 2002, 14, 1325.
13. Kojima, Y.; Usuki, A.; Kawasumi, M.; Okada, A.; Kurauchi, T.; Kamigaito, O. *J Polym Sci Part A: Polym Chem* 1993, 31, 983.
14. Kojima, Y.; Usuki, A.; Kawasumi, M.; Okada, A.; Kurauchi, T.; Kamigaito, O. *J Mater Res* 1993, 8, 1185.
15. Lebaron, P. C.; Wang, Z.; Pinnavia, T. *J Appl Clay Sci* 1999, 15, 11.
16. Moler, K.; Bein, T.; Fisher, R. X. *Chem Mater* 1999, 11, 665.
17. Takashi, K.; Alexander, B. M.; Joseph, M. A.; Mark, R. V.; Richard, H. H.; Walid, H. A.; John, R. S. *J Appl Polym Sci* 2003, 89, 2072.
18. Bourgeat-Lami, E. *J Nanosci Nanotechnol* 2002, 2, 1.
19. Pu, Z. C.; Mark, J. E.; Jethmalani, J. M.; Ford, W. T. *Chem Mater* 1997, 9, 2442.
20. Barthet, C.; Hickey, A. J.; Carrns, D. B.; Armes, S. P. *Adv Mater* 1999, 11, 408.
21. Percy, M. J.; Barthet, C.; Lobb, J. C.; Khan, M. A.; Lasselles, S. F.; Vamvakaki, M.; Armes, S. P. *Langmuir* 2000, 16, 6913.
22. Amalvy, J. I.; Percy, M. J.; Armes, S. P.; Wiese, H. *Langmuir* 2001, 17, 4770.
23. Percy, M. J.; Armes, S. P. *Langmuir* 2002, 18, 4562.
24. Han, M. G.; Armes, S. P. *Langmuir* 2003, 19, 4523.
25. Percy, M. J.; Michailidou, V.; Armes, S. P.; Perruchot, C.; Watts, J. F.; Greaves, S. J. *Langmuir* 2002, 18, 19.
26. Percy, M. J.; Amalvy, J. I.; Randall, D. P.; Armes, S. P.; Greaves, S. J.; Watts, J. F. *Langmuir* 2004, 20, 2184.
27. Tiarks, F.; Landfester, K.; Antonietti, M. *Langmuir* 2001, 17, 5775.
28. Chen, M.; Wu, L.; Zhou, S.; You, B. *Macromolecules* 2004, 37, 9613.
29. Chen, M.; Zhou, S.; You, B.; Wu, L. *Macromolecules* 2005, 38, 6411.
30. Vignati, E.; Piazza, R. *Langmuir* 2003, 19, 6650.
31. Arrighi, V.; McEwen, I. J.; Qian, H.; Serrano Prieto, M. B. *Polymer* 2003, 44, 6259.